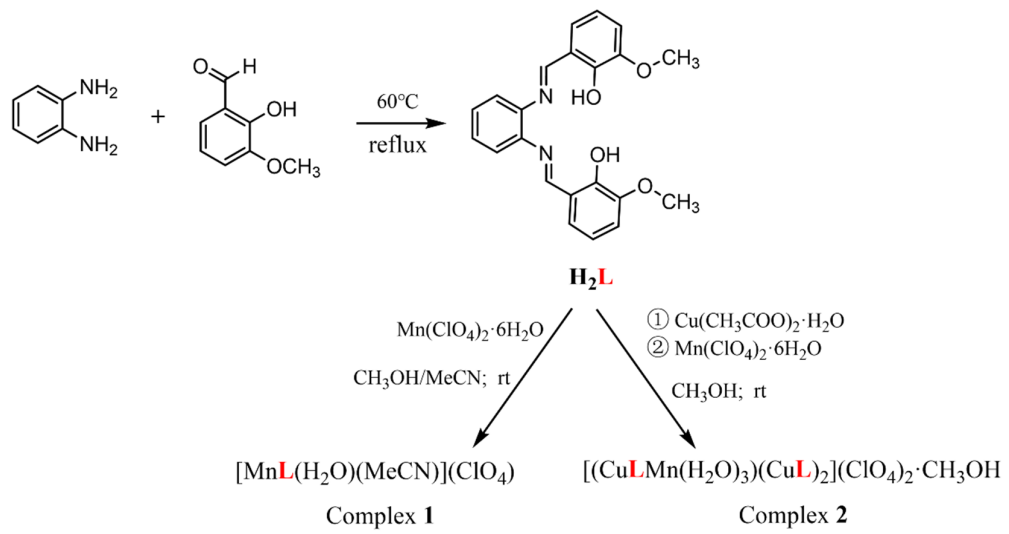


SUPPORTING INFORMATION:

Two Novel Schiff Base Manganese Complexes as Bifunctional Electrocatalysts for CO₂ Reduction and Water Oxidation

Xin Zhao¹, Jingjing Li ², Hengxin Jian ¹, Mengyu Lu ¹, and Mei wang ^{1*}

Contents	Page No
Scheme A1. The synthesis scheme for H ₂ L and the metal complexes 1 and 2 under study.....	2
Figure A1. IR spectrum of the complex 1.....	2
Figure A2. IR spectrum of the complex 2.....	3
Figure A3. The magnetic moment (μ_{eff}) of complex 1	3
Figure A4. In situ UV-vis spectra of complex 1 in DMF:H ₂ O (3:7 v/v) solution containing 0.2 M phosphonate buffer solution at 1.27 V (a) and 1.58 V (b), and in situ UV-vis spectra of complex 2 in DMF:H ₂ O (3:7 v/v) solution containing 0.2 M phosphonate buffer at 1.15 V (c).....	4
Figure A5. Cyclic voltammograms of different concentrations of 0.5 mM complex 1 (a) and 2 (b) in DMF:H ₂ O (3:7 v/v) solution containing 0.2 M phosphonate buffer at optimal pH (scanning rate is 100 mV s ⁻¹). The inset is the relationships of catalytic currents with concentrations.....	4
Figure A6. Cyclic voltammetry of 1 (a) and 2 (b) in DMF under CO ₂ recorded at scan rates range from 100 to 500 mV s ⁻¹ . The inset is the relationships of the peak currents with the square root of the scan rates.	5
Figure A7. Cyclic voltammetry of complexes 1 (a) and 2 (b) in the 0.1 M ⁿ Bu ₄ NPF ₆ DMF solution under CO ₂ in different concentrations (the scanning rate is 100 mV s ⁻¹). The inset is the relationship between complex concentration and reduction peak current.....	5
Figure A8. In situ UV-vis spectra of complex 1 in 0.1 M ⁿ Bu ₄ NPF ₆ DMF at -1.65 V (a) and in situ UV-vis spectra of complex 2 in 0.1 M ⁿ Bu ₄ NPF ₆ DMF solution at -1.60 V (b).....	6
Table A1. Nomenclature table for all the special symbols in the text.	6
Table A2. Comparison of different parameters of the reported similar homogeneous catalysts in recent years. 7	7
Table A3. Crystallographic data and structure correction parameters of complexes 1 and 2.....	7
Table A4. The main key length and key angle of the complex 1 and 2.	8
Table A5. Comparison of different parameters of complexes for water oxidation in recent years.	9
Table A6. Comparison of different parameters of complexes for carbon dioxide reduction in recent years.....	9



Scheme S1. The synthesis scheme for **H₂L** and the metal complexes **1** and **2** under study.

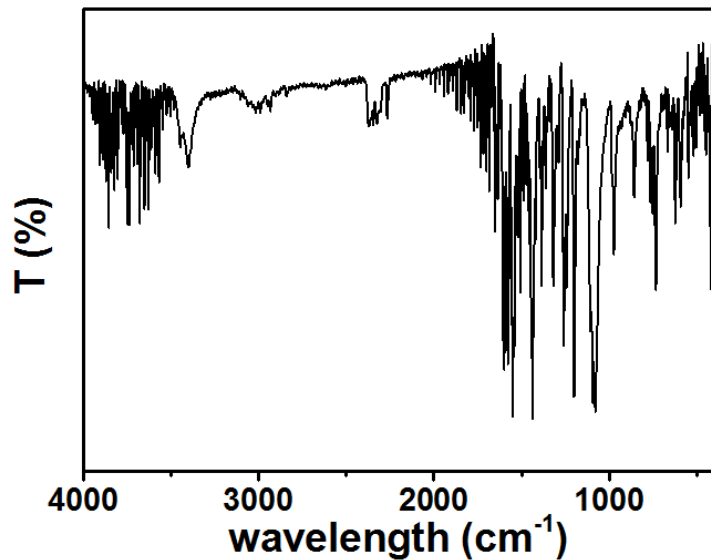


Figure S1. IR spectrum of the complex **1**.

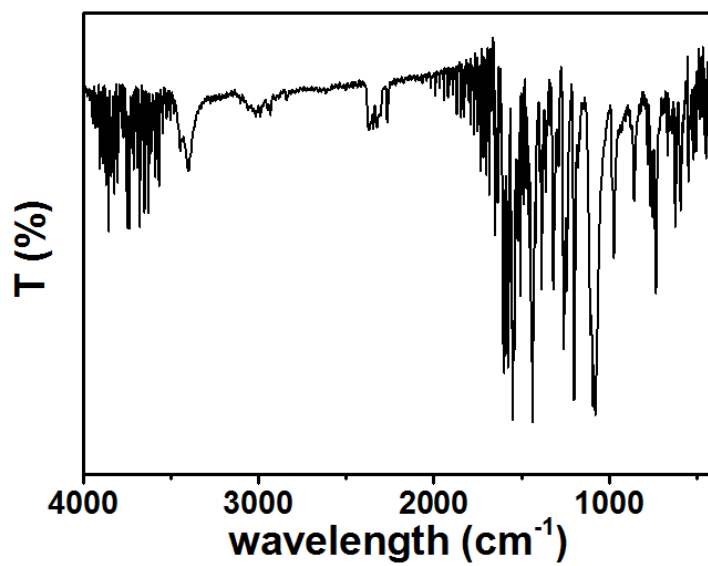


Figure S2. IR spectrum of the complex 2.

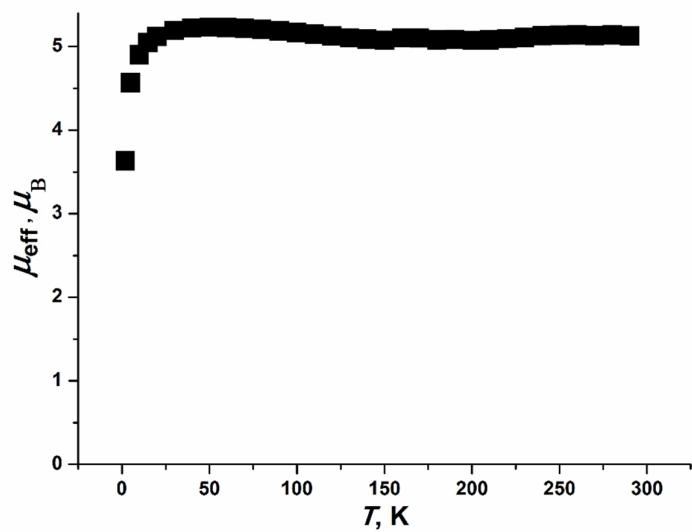


Figure S3. The magnetic moment (μ_{eff}) of complex 1.

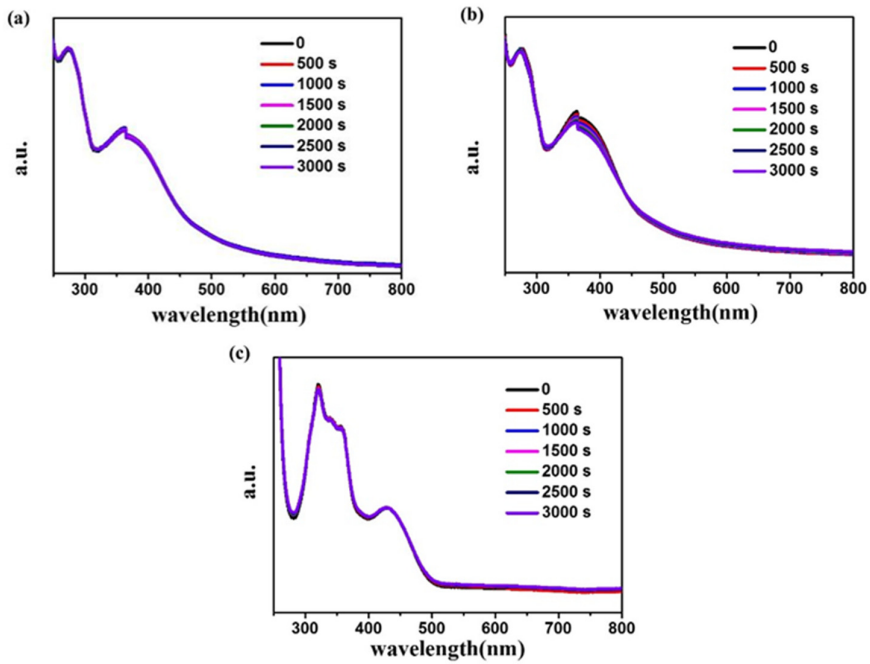


Figure S4. In situ UV-vis spectra of complex **1** in DMF:H₂O (3:7 v/v) solution containing 0.2 M phosphonate buffer solution at 1.27 V **(a)** and 1.58 V **(b)**, and in situ UV-vis spectra of complex **2** in DMF:H₂O (3:7 v/v) solution containing 0.2 M phosphonate buffer at 1.15 V **(c)**.

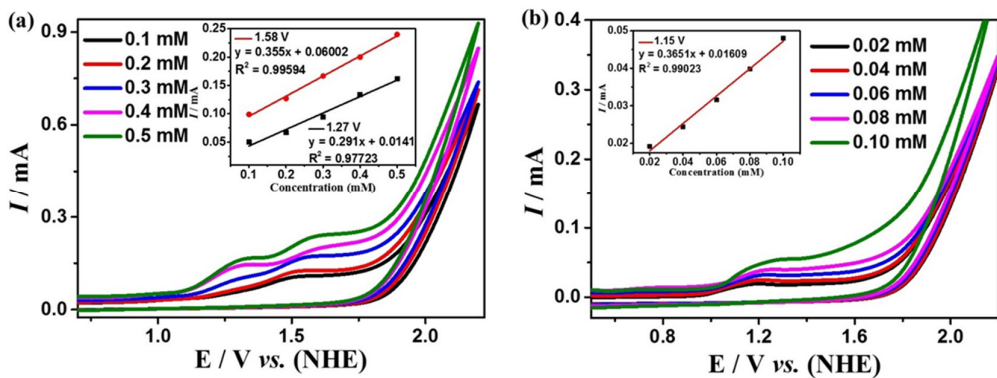


Figure S5. Cyclic voltammograms of different concentrations of 0.5 mM complex **1** **(a)** and **2** **(b)** in DMF:H₂O (3:7 v/v) solution containing 0.2 M phosphonate buffer at optimal pH (scanning rate is 100 mV s⁻¹). The inset is the relationships of catalytic currents with concentrations.

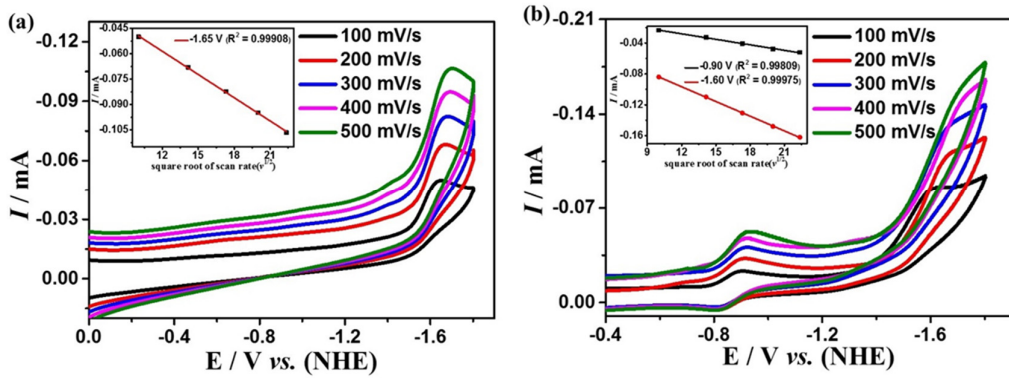


Figure S6. Cyclic voltammetry of **1** (a) and **2** (b) in DMF under CO_2 recorded at scan rates range from 100 to 500 mV s^{-1} . The inset is the relationships of the peak currents with the square root of the scan rates.

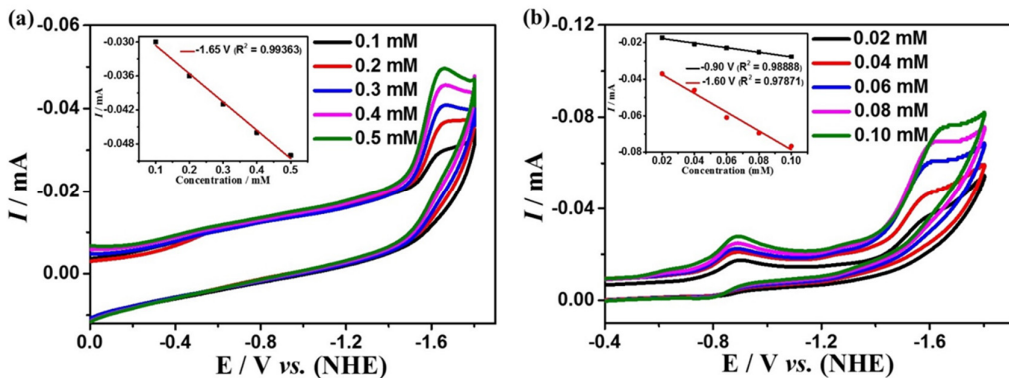


Figure S7. Cyclic voltammetry of complexes **1** (a) and **2** (b) in the 0.1 M ${}^n\text{Bu}_4\text{NPF}_6$ DMF solution under CO_2 in different concentrations (the scanning rate is 100 mV s^{-1}). The inset is the relationship between complex concentration and reduction peak current.

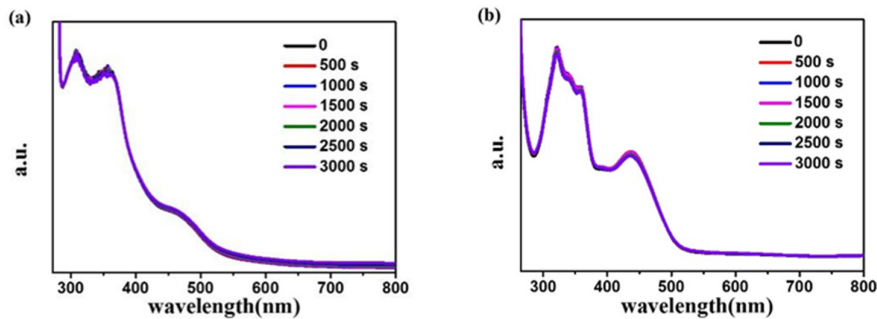


Figure S8. In situ UV-vis spectra of complex **1** in 0.1 M $n\text{Bu}_4\text{NPF}_6$ DMF at -1.65 V **(a)** and in situ UV-vis spectra of complex **2** in 0.1 M $n\text{Bu}_4\text{NPF}_6$ DMF solution at -1.60 V **(b)**.

Table S1. Nomenclature table for all the special symbols in the text.

Abbreviation	Name/Description
Ar	Argon
CV	cyclic voltammogram
CO_2	carbon dioxide
CPE	controlled potential electrolysis
CoFPC	perfluorinated cobalt phthalocyanine
DMF	dimethylformamide
FE	Faradaic efficiency
FTO	F-doped tin oxide
GC	glassy carbon
NHE	normal hydrogen electrode
OER	Oxygen Evolution Reaction
PCET	proton-coupled electron transfer
TOF	turnover frequency
UV-Vis	ultraviolet-visible
F	Faraday constant ($96,485 \text{ C mol}^{-1}$)
i_{cat}	catalytic current
i_p	peak current measured without substrate
n_{cat}	number of electrons involved in the catalytic reaction
n_p	number of electrons participating in the noncatalytic redox reaction ($n_p = 1$)
R	general gas constant ($8.314 \text{ J K}^{-1} \text{ mol}^{-1}$)
T	Kelvin unit temperature
v	scan rate (0.1 V s^{-1})
η	Overpotential
μ_{eff}	magnetic moment

Table S2. Comparison of different parameters of the reported similar homogeneous catalysts in recent years.

catalyst	OER			CO ₂ RR			ref
	FE(%)	η (mV)	TOF(s ⁻¹)	FE(%)	η (mV)	TOF(s ⁻¹)	
[(tpy)(Mebim-py)Ru ^{II} (S)] ²⁺	-	-	-	85	1650	-	[1]
[(^B ⁸ tpy)Ru(phenCO ₂)][PF ₆] ⁻	-	-	-	-	-	-	[2]
[Cu ^{II} L ₂](ClO ₄) ₂ ·2CH ₃ OH	-	-	9.20	-	-	2.99	[3]
(Et ₃ NH) ₂ [Co ^{III} Co ^{II} (OH ₂)(pda) ₅] ⁺	96	233	2.22	9.1	-	0.93	[4]
[Mn ^{III} L(H ₂ O)(MeCN)][ClO ₄] ⁻	88	728	3.66	4	-	0.38	This work
[(Cu ^{II} L ₁ Mn ^{II} (OH ₂) ₃)(Cu ^{II} L ₁) ₂](ClO ₄) ₂ ·CH ₃ OH	92	216	7.88	48	-	15.97	This work

[2] This work only studied the catalytic capability of Ru complex, but with no any quantitative values for catalysis.

Table S3. Crystallographic data and structure correction parameters of complexes **1** and **2**.

Parameter	1	2
Chemical formula	C ₂₄ H ₂₃ ClMnN ₃ O ₉	C ₆₇ H ₆₄ Cl ₂ Cu ₃ MnN ₆ O ₂₄
Formula weight	587.84	1653.70
Crystal system	Monoclinic	Triclinic
space group	P121/c1	P-1
a (Å)	10.4754(13)	13.620(2)
b (Å)	16.4898(19)	20.403(3)
c (Å)	14.7342(16)	26.782(3)
α (°)	90	91.533(4)
β (°)	110.019(3)	91.052(6)
γ (°)	90	92.062(5)
V (Å ³)	2391.4(5)	7433.8(18)
Z	4	4
ρ_{calcd} (g m ⁻³)	1.633	1.478
μ (mm ⁻¹)	0.726	1.164
Reflections collected	9034	70702
F(000)	1208.0	3384.0
R _{int}	0.0601	0.0741
T (K)	170	170
Final R indices	R ₁ = 0.0546	R ₁ = 0.1179
[I > 2sigma(I)]	wR ₁ = 0.1457	wR ₁ = 0.3161
R indices (all data)	R ₂ = 0.0814	R ₂ = 0.1490
	wR ₂ = 0.1729	wR ₂ = 0.3345
Gof	1.135	1.041

Table S4. The main key length and key angle of the complex **1** and **2**.

bond	d. Å	bond	d. Å
complex 1			
Mn(01)-O(1)	2.257(2)	Mn(01)-N(2)	1.973(3)
Mn(01)-O(3)	1.863(2)	Mn(01)-N(1)	1.978(3)
Mn(01)-O(2)	1.868(2)	Mn(01)-N(3)	2.380(4)
complex 2			
Cu(6)-O(26)	1.900(7)	Cu(3)-O(14)	1.876(7)
Cu(6)-N(11)	1.895(9)	Cu(3)-N(6)	1.911(11)
Cu(6)-O(25)	1.876(8)	Cu(3)-N(5)	1.940(9)
Cu(6)-N(12)	1.935(9)	Cu(4)-O(16)	1.875(8)
Cu(1)-O(2)	1.918(8)	Cu(4)-N(7)	1.953(10)
Cu(1)-O(1)	1.900(8)	Cu(4)-N(8)	1.949(9)
Cu(1)-N(1)	1.950(10)	Cu(4)-O(17)	1.890(8)
Cu(1)-N(2)	1.918(9)	Mn(1)-O(5)	2.216(7)
Cu(2)-O(5)	1.840(7)	Mn(1)-O(11)	2.119(9)
Cu(2)-O(6)	1.908(7)	Mn(1)-O(6)	2.183(8)
Cu(2)-N(4)	1.899(9)	Mn(1)-O(7)	2.117(8)
Cu(2)-N(3)	1.895(10)	Mn(1)-O(9)	2.163(11)
Cu(5)-O(21)	1.867(7)	Mn(2)-O(21)	2.209(7)
Cu(5)-O(20)	1.923(8)	Mn(2)-O(00J)	2.147(8)
Cu(5)-N(9)	1.875(9)	Mn(2)-O(20)	2.142(8)
Cu(5)-N(10)	1.937(11)	Mn(2)-O(015)	2.109(9)
Cu(3)-O(12)	1.899(7)	Mn(2)-O(22)	2.132(9)

Angle	ω , deg	Angle	ω , deg
complex 1			
O(1)-Mn(01)-N(3)	178.05(9)	O(2)-Mn(01)-N(1)	93.18(11)
O(3)-Mn(01)-O(1)	92.21(9)	O(2)-Mn(01)-N(3)	90.85(10)
O(3)-Mn(01)-O(2)	91.37(9)	N(2)-Mn(01)-O(1)	93.00(10)
O(3)-Mn(01)-N(2)	93.05(9)	N(2)-Mn(01)-N(1)	82.35(11)
O(3)-Mn(01)-N(1)	175.29(10)	N(2)-Mn(01)-N(3)	86.91(11)
O(3)-Mn(01)-N(3)	89.74(10)	N(1)-Mn(01)-O(1)	89.05(10)
O(2)-Mn(01)-O(1)	89.09(10)	N(1)-Mn(01)-N(3)	89.01(11)
O(2)-Mn(01)-N(2)	175.03(11)		
complex 2			
O(26)-Cu(6)-N(12)	94.9(4)	O(14)-Cu(3)-N(5)	176.8(4)
N(11)-Cu(6)-O(26)	178.7(4)	N(6)-Cu(3)-N(5)	84.4(4)
N(11)-Cu(6)-N(12)	84.0(4)	O(16)-Cu(4)-N(7)	176.8(4)
O(25)-Cu(6)-O(26)	87.9(3)	O(16)-Cu(4)-N(8)	93.4(4)
O(25)-Cu(6)-N(11)	93.1(4)	O(16)-Cu(4)-O(17)	88.2(4)
O(25)-Cu(6)-N(12)	176.7(4)	N(8)-Cu(4)-N(7)	84.7(4)
O(2)-Cu(1)-N(1)	178.7(4)	O(17)-Cu(4)-N(7)	93.5(4)
O(1)-Cu(1)-O(2)	88.7(4)	O(17)-Cu(4)-N(8)	176.4(4)
O(1)-Cu(1)-N(1)	92.3(4)	O(11)-Mn(1)-O(5)	94.0(3)
O(1)-Cu(1)-N(2)	176.4(4)	O(11)-Mn(1)-O(6)	90.8(3)
N(2)-Cu(1)-O(2)	94.3(4)	O(11)-Mn(1)-O(9)	86.0(4)
N(2)-Cu(1)-N(1)	84.7(4)	O(6)-Mn(1)-O(5)	69.1(2)

O(5)-Cu(2)-O(6)	83.4(3)	O(7)-Mn(1)-O(5)	89.5(3)
O(5)-Cu(2)-N(4)	178.2(4)	O(7)-Mn(1)-O(11)	176.4(3)
O(5)-Cu(2)-N(3)	95.5(4)	O(7)-Mn(1)-O(6)	90.3(3)
N(4)-Cu(2)-O(6)	97.1(4)	O(7)-Mn(1)-O(9)	91.1(4)
N(3)-Cu(2)-O(6)	178.6(4)	O(9)-Mn(1)-O(5)	148.2(3)
N(3)-Cu(2)-N(4)	84.0(4)	O(9)-Mn(1)-O(6)	142.7(3)
O(21)-Cu(5)-O(20)	81.7(3)	O(00J)-Mn(2)-O(21)	92.3(3)
O(21)-Cu(5)-N(9)	176.9(3)	O(20)-Mn(2)-O(21)	69.5(3)
O(21)-Cu(5)-N(10)	97.0(4)	O(20)-Mn(2)-O(00J)	93.3(3)
O(20)-Cu(5)-N(10)	178.2(4)	O(015)-Mn(2)-O(21)	90.3(3)
N(9)-Cu(5)-O(20)	96.4(3)	O(015)-Mn(2)-O(00J)	176.5(3)
N(9)-Cu(5)-N(10)	84.8(4)	O(015)-Mn(2)-O(20)	89.8(3)
O(12)-Cu(3)-N(6)	177.5(4)	O(015)-Mn(2)-O(22)	87.8(4)
O(12)-Cu(3)-N(5)	93.6(4)	O(22)-Mn(2)-O(21)	143.8(3)
O(14)-Cu(3)-O(12)	88.5(3)	O(22)-Mn(2)-O(00J)	88.8(3)
O(14)-Cu(3)-N(6)	93.5(4)	O(22)-Mn(2)-O(20)	146.6(3)

Table S5. Comparison of different parameters of complexes for water oxidation in recent years.

catalyst	η (mV)	TOF(s ⁻¹)	ref
[Cu ₂ (TPMAN)(μ-OH)](CF ₃ SO ₃) ₃	780	0.78	[5]
[Cu(I)(MePzPy)]PF ₆	674	9.77	[6]
6-FP-Co-OMC-1	400	0.53	[7]
C30H38N4Rh ₂ Cl	325	0.8	[8]
[(Cu ^{II} L ₁ Mn ^{II} (OH ₂) ₃)(Cu ^{II} L ₁) ₂](ClO ₄) ₂ ·CH ₃ OH	216	7.88	This work

Table S6. Comparison of different parameters of complexes for carbon dioxide reduction in recent years.

catalyst	TOF(s ⁻¹)	ref
[W(bpy-H)(CO) ₄]	0.002	[9]
NiPcP	6.43	[10]
3D-Por(Co/H)-COF	1.28	[11]
Cr(^{tbu} dhbipy)Cl(H ₂ O)	5.7	[12]
[Ni(qlca)Cl ₂]	0.83	[13]
(Et ₃ N) ₂ [CoII ₂ CoI(OH ₂)(pda) ₅]·H ₂ O	0.93	[4]
[(Cu ^{III} L ₁ Mn ^{II} (OH ₂) ₃)(Cu ^{III} L ₁) ₂](ClO ₄) ₂ ·CH ₃ OH	15.97	This work

References

- Chen, Z.F.; Concepcion, J.J.; Brennaman, M.K.; Kang, P.; Norris, M.R.; Hoertz, P.G.; Meyer, T.J. Splitting CO₂ into CO and O₂ by a single catalyst. *PNAS* **2012**, 109, 15606-15611.
- Das, B.; Ezzedinloo, L.; Bhadbhade, M.; Bucknall, M.P.; Colbran, S.B. Strategic design of a ruthenium catalyst for both CO₂ reduction and H₂O oxidation: the electronic influence of the co-ligands. *Chem. Commun.* **2017**, 53, 10006.

3. Shi, N.N.; Xie, W.J.; Zhang, D.M.; Fan, Y.H.; Cui, L.S.; Wang, M. A mononuclear copper complex as bifunctional electrocatalyst for CO₂ reduction and water oxidation. *J. Electroanal. Chem.* **2021**, 886, 115106.
4. Yin, X.M.; Zhang, S.F.; Wang, J.M.; Li, J.J.; Chen, F.F.; Yao, S.; Fan, Y.H.; Wang, M. Bioinspired cobalt molecular electrocatalyst for water oxidation coupled with carbon dioxide reduction. *Appl. Organomet. Chem.* **2021**, 35, e6371.
5. Hu, Q.Q; Su, X.J; Zhang, M.T. Electrocatalytic Water Oxidation by an Unsymmetrical Di-Copper Complex. *Inorg. Chem.* **2018**, 57, 10481-10484.
6. Makhado, T.; Das, B.; Kriek, R. J.; Vosloo, H. C. M.; Swarts, A. J. Chemical and electrochemical water oxidation mediated by bis(pyrazol-1-ylmethyl)pyridine-ligated Cu(I) complexes. *Sustain. Energ. Fuels* **2021**, 5, 2771-2780.
7. Liu, C.; Geer, Ana M.; Webber, C.; Musgrave, C.B.; et.al Immobilization of “Capping Arene” Cobalt(II) Complexes on Ordered Mesoporous Carbon for Electrocatalytic Water Oxidation. *ACS Catal.* **2021**, 11, 15068-15082.
8. Li, P.; Liu, J.B; Han, S.; Deng, W.; Yao, Z.J. Half-sandwich Ir (III) and Rh (III) complexes as catalysts for water oxidation with double-site. *Appl. Organomet. Chem.* **2019**, 33.
9. Li, X.H.; Panetier, J.A. Mechanistic Study of Tungsten Bipyridyl Tetracarbonyl Electrocatalysts for CO₂ Fixation: Exploring the Roles of Explicit Proton Sources and Substituent Effects. *Top. Catal.* **2022**, 65, 325-340.
10. Wei, S.T.; Zou, H.Y.; Rong, W.F.; Zhang, F.X.; Ji, Y.F; Duan, L.L. Conjugated nickel phthalocyanine polymer selectively catalyzes CO₂-to-CO conversion in a wide operating potential window. *Appl. Catal. B* **2021**, 284, 119739.
11. Chi, S.Y.; Chen, Q.; Zhao, S.S.; Si, D.H.; Wu, Q.J.; Huang, Y.B.; Cao, R. Three-dimensional porphyrinic covalent organic frameworks for highly efficient electroreduction of carbon dioxide. *J. Mater. Chem. A* **2022**, 10, 4653-4659.
12. Hooe, S.L.; Dressel, J.M.; Dickie, D.A.; Machan, C.W. Highly Efficient Electrocatalytic Reduction of CO₂ to CO by a Molecular Chromium Complex. *ACS Catal.* **2020**, 10, 1146-1151.
13. Ahsan, H.Md.; Breedlove, B.K.; Piangrawee, S.; Mian, M.R.; Fetoh, A.; Cosquer, G.; Yamashita, M. Enhancement of electrocatalytic abilities for reducing carbon dioxide: functionalization with a redox-active ligand-coordinated metal complex. *Dalton. T.* **2018**, 47, 11313-11316.